Magnetic Field Analysis and Structural Optimization of Deflection Double Stator Switched Reluctance Generator

Zheng Li, Xuze Yu, Xin Wang, Zhe Qian, and Qunjing Wang

Abstract Switched reluctance generator has been widely used in industry. With the consumption of energy, the requirement of generator is higher and higher. The energy conversion rate of the traditional generator structure is very low, and it can no longer meet the existing technical indicators. In order to solve the problem of low efficiency of existing generators, this paper proposes a deflectable double stator switched reluctance generator (DDSRG), and performed a finite element analysis on this model. The magnetic density of the new generator is analyzed. A comparison between the proposed mathematical model and the finite element method verifies the accuracy of the model. finally, the core loss was used as the target to optimize the structure of the generator using the response surface method. The experimental results were compared with the simulation. The error was within the allowable range, which verified the correctness of the calculation method and the optimization scheme.

Keywords Switched reluctance generator · Finite element · Core loss · Response surface method

1 Introduction

Switched reluctance generators have very reliable performance and have been widely used in the industrial field. Compared with other types of generators, switched reluctance generators have a smaller size. At the same time, the two stators of the switched reluctance generator with dual stator structure can simultaneously induce output voltage, which is more suitable for industrial production [1]. To further improve the working efficiency of the generator, the concept of multiple degrees of freedom can be combined with the generator structure. The deflectable generator structure can

Z. Li (✉) · X. Yu · X. Wang
School of Electrical Engineering, Hebei University of Science and Technology, No. 26 Yuxiang street, Yuhua District, Shijiazhuang, Hebei Province, China
e-mail: Lzhfgd@163.com

Z. Qian · Q. Wang
National Engineering Laboratory of Energy-Saving Motor and Control Technique, No. 111 Jiulong Road, Shushan District, Hefei, Anhui Province, China

W. Chen et al. (eds.), *The Proceedings of the 9th Frontier Academic Forum of Electrical Engineering*, Lecture Notes in Electrical Engineering 743,
https://doi.org/10.1007/978-981-33-6609-1_56

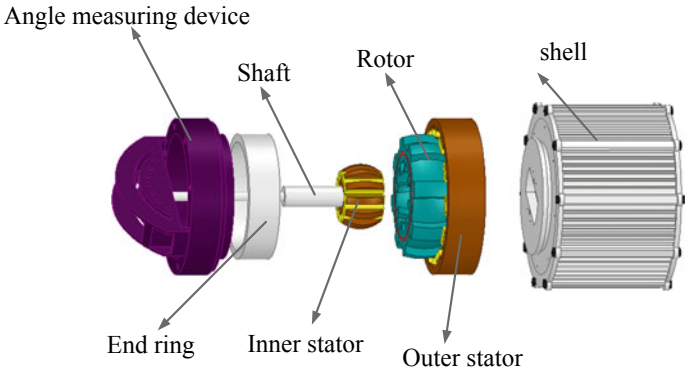

Fig. 1 Structure of deflected double stator generator

improve the power generation efficiency of the generator. Although the dual-stator structure generator has better power generation characteristics, at the same time its iron loss will also increase to a greater extent. This is not negligible for a switched reluctance motor with a double stator structure [2].

This paper proposes a mathematical model for the proposed new generator structure, and compares the test results with the finite element results to verify the accuracy of the model. Finally, the analysis and optimization results are verified through experiments.

2 Structure and Principle of DDSRG

The structure model of DDSRG is shown in Fig. 1. Both stator and rotor are spherical in shape. The parameters of the generator are shown in Table 1.

The tooth pole axis of the inner stator is consistent with that of the outer stator. DDSRG can be regarded as a combination of an inner generator and an outer generator, with a rotor between the inner and outer stators.The rotor part has a magnetic isolation part, which can isolate the magnetic fields of the inner and outer stators from each other.

3 Analytical Calculation of Magnetic Density of DDSR

The magnetic field strength of the main air gap magnetic field, the magnetic density of the main air gap magnetic field, and the magnetic density of the edge air gap magnetic field can be expressed by Eqs. (1)–(3), respectively.

Table 1 Structural parameters of generator

Parameter	Value
Outer stator radius/mm	120
Inner stator radius/mm	19.45
Rotor inner diameter/mm	40.31
Rotor outer diameter/mm	85.5
Inner and outer air gap/mm	1.5
Number of stator teeth	12
Number of rotor teeth	8
Stator pole arc/°	14.9
Rotor pole arc/°	16.1
Core length/mm	60
Unidirectional deflection range/°	0–17

$$H_m = \frac{B_s\left(2\mu_r l_g + 2l_g + l + 2ll_g\right) + N_m i_m \mu_0 \mu_r \left(l + l_g\right)}{2\mu_0 \mu_r l l_g} - \sqrt{\left(\frac{B_s\left(2\mu_r l_g + 2l_g + l + 2ll_g\right) + N_m i_m \mu_0 \mu_r \left(l + l_g\right)}{2\mu_0 \mu_r l l_g}\right)^2 - \frac{N_m i_m \left[B_s\left(\mu_r l - \mu_r l_g + l - l_g\right) + \mu_0 \mu_r N_m i_m\right]}{\mu_0 \mu_r l}} \tag{1}$$

$$B_m = \frac{B_s\left(2\mu_r l_g + 2l_g + l + 2ll_g\right) + N_m i_m \mu_0 \mu_r \left(l + l_g\right)}{2\mu_r l l_g} - \sqrt{\left(\frac{B_s\left(2\mu_r l_g + 2l_g + l + 2ll_g\right) + N_m i_m \mu_0 \mu_r \left(l + l_g\right)}{2\mu_r l l_g}\right)^2 - \frac{\mu_0 N_m i_m \left[B_s\left(\mu_r l - \mu_r l_g + l - l_g\right) + \mu_0 \mu_r N_m i_m\right]}{\mu_r l}} \tag{2}$$

$$B_{\mathrm{f}} = \frac{2\mu_0 \mu_r N_{\mathrm{m}} i_{\mathrm{m}} \left(\frac{A_{\mathrm{s}}}{l - l_{\mathrm{f}}} + A_{\mathrm{f}}\right) + B_{\mathrm{s}}(A_{\mathrm{s}} l_{\mathrm{f}} \mu_r + A_{\mathrm{s}} l_{\mathrm{f}} + A_{\mathrm{f}} l - A_{\mathrm{f}} l_{\mathrm{f}}) - \Phi_{\mathrm{m}} \mu_0 \mu_r l_{\mathrm{f}}}{2\mu_{\mathrm{r}} l_{\mathrm{f}} N_{\mathrm{m}} i_{\mathrm{m}} \left(\frac{A_{\mathrm{s}}}{l - l_{\mathrm{f}}} + 2A_{\mathrm{f}}\right)} - \sqrt{\left(\frac{2\mu_0 \mu_r N_{\mathrm{m}} i_{\mathrm{m}} \left(\frac{A_{\mathrm{s}}}{l - l_{\mathrm{f}}} + A_{\mathrm{f}}\right) + B_{\mathrm{s}} l_{\mathrm{f}} (A_{\mathrm{s}} \mu_r + A_{\mathrm{s}}) - \Phi_{\mathrm{m}} \mu_0 \mu_r l_{\mathrm{f}}}{2\mu_{\mathrm{r}} l_{\mathrm{f}} N_{\mathrm{m}} i_{\mathrm{m}} \left(\frac{A_{\mathrm{s}}}{l - l_{\mathrm{f}}} + 2A_{\mathrm{f}}\right)}\right)^2 - \frac{A_{\mathrm{s}} \left(\frac{\mu_0 \mu_r A_{\mathrm{s}} N_{\mathrm{m}} i_{\mathrm{m}}}{l - l_{\mathrm{f}}} + B_{\mathrm{s}} N_{\mathrm{m}} i_{\mathrm{m}} \mu_r\right) - \Phi_{\mathrm{m}} (\mu_0 \mu_r N_{\mathrm{m}} i_{\mathrm{m}} + B_{\mathrm{s}} l - B_{\mathrm{s}} l_{\mathrm{f}})}{\mu_r l_{\mathrm{f}} N_{\mathrm{m}} i_{\mathrm{m}} \left(\frac{A_{\mathrm{s}}}{l - l_{\mathrm{f}}} + 2A_{\mathrm{f}}\right)}} \tag{3}$$

where A_{f1} and A_{f2} are the areas where the lines of force pass through the edges on both sides. $A_f = A_{f1} + A_{f2}$, lf is the average length of the edge magnetic circuit on both sides, l_g is the average air gap length, N_m is the number of turns of the outer stator winding, i_m is the phase current of the winding. B_s is the saturation magnetic density of the material.

4 Finite Element Analysis Results of Generator Magnetic Field

The deflection type double stator switched reluctance generator can be composed of the radial component Br and the tangential component B_θ [3–6].

In the transient field, the composite flux density and magnetic flux density components of each element are simulated. The analysis radius of the outer rotor yoke is 55–70 mm. The analysis radius of the outer rotor teeth is from 70 to 75 mm. The analysis radius of outer stator teeth is 75.5–80.5 mm. The analysis radius of the outer stator yoke is 80.5–110 mm. Figure 2 shows the changes in the magnetic density of different types of generators.

The error between the analytical method and the finite element method is relatively small enough.

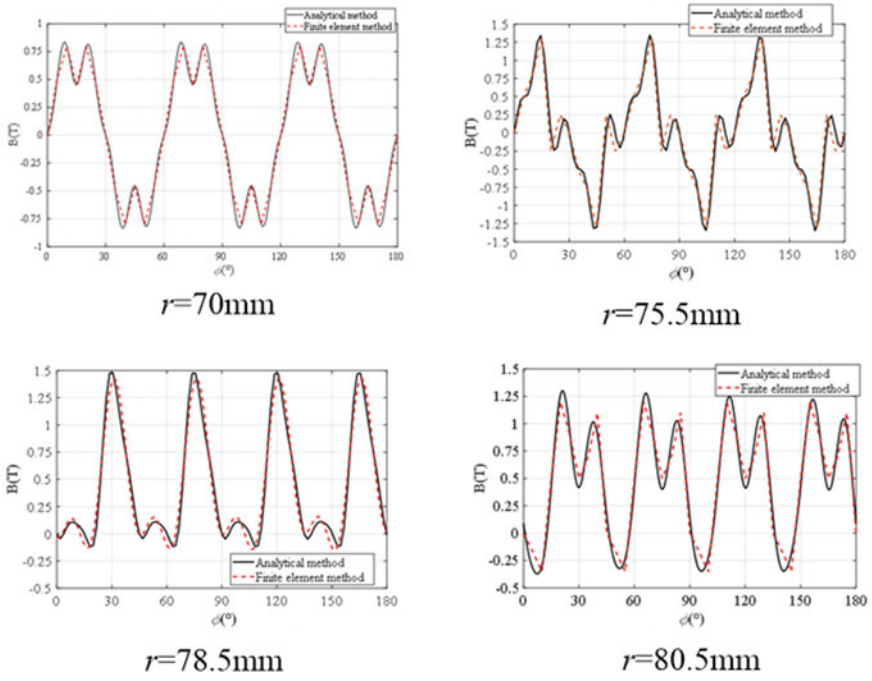

Fig. 2 Comparison of magnetic flux density by analytical method and FEM

5 Structural Optimization of DDSRG

Bertotti et al. believe that the core loss is mainly composed of three types of loss, namely eddy current loss, eddy current loss P_e, hysteresis loss P_h, and residual loss. P_c [7, 8].

$$P_{\mathrm{Fe}} = P_{\mathrm{e}} + P_{\mathrm{h}} + P_{\mathrm{c}} \tag{4}$$

The change of stator and rotor structure has a great influence on hysteresis loss.

Four design variables are selected: core length L_1, stator outer pole width B_1, stator outer yoke height $H1$ and outer air gap G_1.

Figure 3 is the schematic diagram of generator optimization parameters. Each optimized parameter has 3 value variables, respectively, the values of the A, B, and C variables determine the changes of the four parameters. The changes of the four parameters are shown in Table 2.

Taguchi algorithm helps to greatly reduce the iterative method in the experiment and reduce the cost of the experiment [9]. The core loss of the generator model is analyzed using finite element, and the core loss P_{Fe} of each combination in the orthogonal table is obtained, as shown in Table 3.

Table 3 is the orthogonal experiment table, and the finite element method can be used to calculate the iron loss under different conditions.

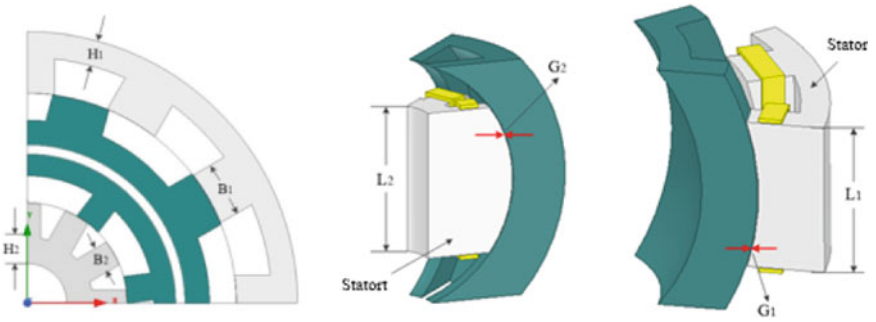

Fig. 3 Generator optimization parameters

Table 2 The optimized parameters and evaluated parameters

Optimization parameters	L_1/mm	B_1/mm	$H1$/mm	G_1/mm
A	60	26	12	0.1
B	75	33	15	0.5
C	90	40	18	0.9

Table 3 Analysis results

	L_1/mm	B_1/mm	$H1$/mm	G_1/mm	P_{Fe}/W
1	A	A	A	A	276.0
2	A	B	B	B	234.6
3	A	C	C	C	172.2
4	B	A	C	C	237.0
5	B	B	B	A	150.0
6	B	C	A	B	212.4
7	C	A	C	B	280.2
8	C	B	A	C	250.8
9	C	C	B	A	156.0

$$YY = 3\sum_{i=1}^{3}[m_{xi}(P_{\mathrm{Fe}i}) - m(P_{\mathrm{Fe}})]^2 \tag{5}$$

where YY is the proportion of each parameter variable affecting the performance, x is the optimized parameter variable, namely the core length L_1, the outer stator pole width B_1, the outer stator yoke height $H1$, the external air gap G_1, m_{xi} (P_{Fei}) as the parameters The average value of the core loss of the variable x under the i-th level variable, $m(P_{Fe})$ is the average value of P_{Fe} in 9 experiments [10].

As shown in Table 4, the iron loss has a great correlation with the proposed parameters. Among them, the iron core length L_1 accounts for 7.04%, which has a small influence on the iron loss, and the influence rate of other structural parameters is very high. The largest part of the outer stator pole width B_1 accounts for 46.93% of the total proportion.

The outer stator pole width B_1, the outer stator yoke height $H1$, the outer air gap G_1 as the three parameter variables, the core loss of the generator as the response value, the application of the central composite design (CCD) method to obtain the coding con-version of the parameter variables is shown in Table 5.

The data is fitted by the least square method, and based on the results of the response surface, the regression equations with the generator core loss as the response value are obtained as

Table 4 The Influence rate of optimization parameters on generator core loss

Optimization parameters	YY	Impact rate (%)
L1/mm	1627.44	7.04
G1/mm	3520.32	15.23
H1/mm	7118.16	30.80
B1/mm	10,845.96	46.93
Total	23,111.88	100

Table 5 Comparison of measured and calculated values of generator iron loss

Area	Experimental measurement	Simulation calculated value
Internal iron loss/W	54.34	52.80
External iron loss/W	86.87	79.75
Total iron loss/W	141.21	131.55

$$\begin{aligned} Y = {} & 272.52 + 73.68X_1 - 22.70X_2 - 29.08X_3 \\ & + 12.93X_1X_2 - 17.62X_1X_3 + 0.10X_2X_3 \\ & - 19.53X_1^2 - 11.57X_2^2 - 28.93X_3^2 \end{aligned} \tag{6}$$

where X_1 is the outer stator pole width B_1, X_2 is the outer stator yoke height $H1$, and X_3 are the external air gap G_1, where $X_1, X_2, X_3, X_1X_2, X_1X_3, X_{12}, X_{22}$, and X_{32} have a significant effect on the core loss of the generator Significant influence, other items are not significant.

It can be seen from Fig. 4 that the outer stator pole width B_1, the outer stator yoke height $H1$, and the outer air gap G_1 have a significant effect on the response value of the generator core loss.

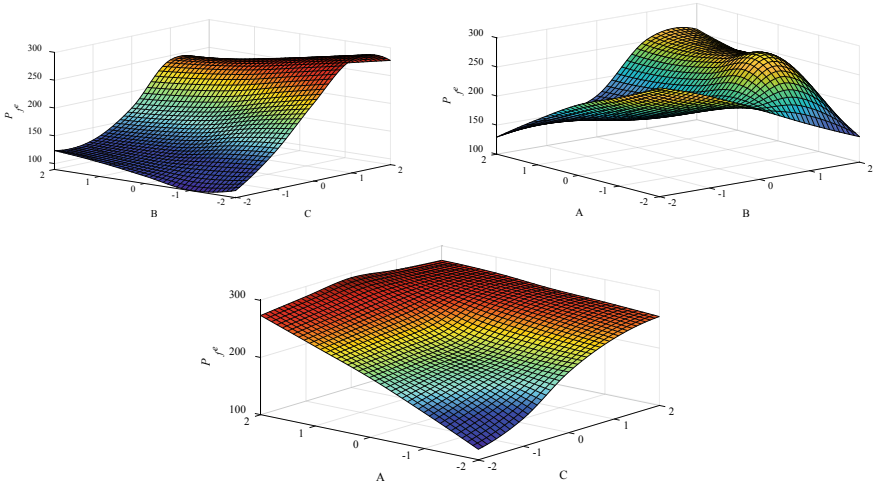

Fig. 4 The relationship between response surface and parameters

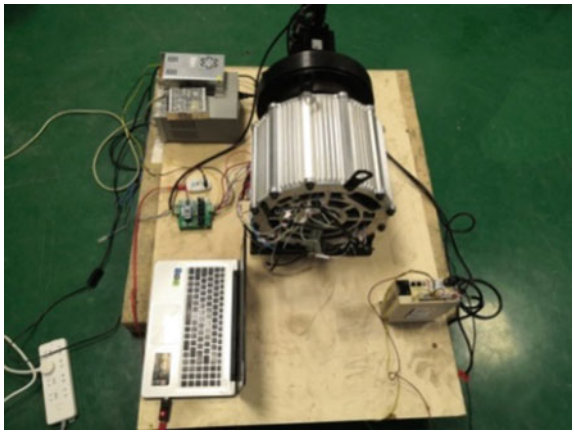

Fig. 5 Experimental device

6 Experimental Verification

When the DDSRG is running in a steady state of rotation, The loss can be calculated by formula (7):

$$P_{\mathrm{Fe}} = P_1 - P_2 - P_{\mathrm{Cu}} - P_{\mathrm{fw}} - P_{\mathrm{s}} \tag{7}$$

where P_1 is input power, P_2 is output power, P_{Cu} is copper loss, P_{fw} is mechanical loss, and P_s represents stray loss. As shown in Fig. 5, the experiment plat-form is composed of generator, power converter and oscilloscope.

7 Conclusion

The deflection type DDSRG has important application value. This paper introduces the basic structure and control principle of the generator, focusing on the magnetic density distribution of the DDSRG under the rotation state. The overall qualitative analysis of the core magnetic density is carried out by using FEM. According to the calculation result of the magnetic density, the Fourier transform is performed to calculate the Iron loss of the DDSRG, and the response surface method is used to optimize the structural parameters of the DDSRG. The indirect measured experimental data verifies the accuracy of the optimization scheme. It provides theoretical support for the subsequent research of the generator.

Acknowledgements This work was supported by the National Natural Science Foundation of China, grant No. 51877070, 51577048, 51637001, the Natural Science Foundation of Hebei Province of China, grant No. E2018208155, the Talent Engineering Training Support Project of Hebei Province, grant No. A201905008, the National Engineering Laboratory of Energy-saving

Motor and Control Technique, Anhui University, grant No. KFKT201901, Hebei Province Higher Education Science and Technology Research Key Project, grant No. ZD2018228.

References

1. Zhou, Yunhong, and Yukun Sun. 2015. A double-stator type bearingless switched reluctance dual-channel full-period generator. *Proceedings of the CSEE* 35 (9): 2295–2303 (in Chinese).
2. Liu, Yongzhi, Zheng Zhou, and Zengjin Sheng. 2015. Research on switching reluctance motor start/power generation switching control strategy. *Electric Machines and Control* 19 (10): 57–63 (in Chinese).
3. Dong, Chuanyou, Yong Li, and Shuye Ding. 2015. Core loss analysis of switched reluctance motor. *Electric Machines and Control* 19 (07): 58–65 (in Chinese).
4. Li, Zheng, Yue Zhang, Qunjing Wang, et al. 2013. Analytical modeling and analysis of magnetic field for a novel 3-DOF deflection type PM motor. *Proceedings of the CSEE* 33 (S1): 219–225 (in Chinese).
5. Tian, Jing, Xuezhong Zhu, and Xiang Zhou. 2015. Analysis and calculation of iron loss of switched reluctance motor. *Mechanical & Electrical Engineering* 32 (2): 256–260 (in Chinese).
6. Narita, K., T. Asanuma, K. Semba, et al. 2015. An accurate iron loss evaluation method based on finite element analysis for switched reluctance motors. In *Energy conversion congress & exposition*. IEEE
7. Heidarian, M., and B. Ganji. 2016. A dynamic simulation model based on finite element method for switched reluctance generator. In *2016 International symposium on power electronics, electrical drives, automation and motion (SPEEDAM)*. IEEE
8. Xu, T., J. Yuan, Q. Wang, et al. 2016. Inductance estimation method for linear switched reluctance machines considering iron losses. *IET Electric Power Applications* 10 (3): 181–188.
9. Cheng, C., F.T. Bao, and H. Xu. 2014. Optimization design for contour of pintle nozzle in solid rocket motor based on response surface method. *Advanced Materials Research* 1016 (1016): 6.
10. Li, Zheng, Zhang Lu, Qunjing Wang, et al. 2015. Optimal design of structure parameters of three-DOF deflection type PM motor based on response surface methodology. *Transactions of China Electrotechnical Society* 30 (13): 134–142 (in Chinese).